ECCOMAS Congress 2016
VII European Congress on Computational Methods in Applied Sciences and Engineering
M. Papadrakakis, V. Papadopoulos, G. Stefanou, V. Plevris (eds.)
Crete Island, Greece, 5–10 June 2016

EFFECTIVE 3D REGULARIZED XFEM FOR PULL-OUT OF STEEL BARS IN CONCRETE, BENDING AND SHEAR TESTS ON FRP-REINFORCED CONCRETE BEAMS

Elena Benvenuti[1*], **Nicola Orlando**[1]

[1] Università di Ferrara, Dipartimento di Ingegneria
address Via Saragat 1, I-44122 Ferrara, Italy
e-mail: elena.benvenuti@unife.it, nicola.orlando@unife.it
ph. nr. +39 0532 974935

Keywords: Delamination, debonding, 3-Dimensional Finite element analysis, XFEM

Abstract. *We present an effective three-dimensional tool for modeling the influence on the structural behavior of the mechanical behavior of the interface between steel bars and FRP plates glued to concrete beams. The proposed tool reproduces the pull out of the bars and the detachment of the FRP plates. Both opening and sliding of the interface between reinforcements and beam are accounted for. The tool is based on the regularized extended finite element method (XFEM) developed by the authors: the discontinuities are regularized and a mechanically consistent variational formulation is adopted. The considered cases range from the simulation of pull-out tests of steel rebars, to the simulation of single-lap tests in shear and three point bending tests in FRP-reinforced concrete beams.*

1 INTRODUCTION

This contribution deals with the modeling of the influence of steel bars and FRP external reinforcements on the structural behavior of concrete beams. We present an original three-dimensional effective tool for modeling the detachment of steel and FRP plates from concrete beams. The proposed extended finite element model is capable of reproducing the pull out of steel bars and the detachment of the FRP-concrete layer taking into account both opening and sliding at the interface between the reinforcements and the concrete. The approach adopted in the present analysis is original, and is based on a recently developed 3D procedure [1] extending the previous 2D formulation for cohesive-like interfaces [2, 3]. The approach can be regarded as an original variant of the widely known eXtended Finite Element Method (XFEM) [4]. In the present XFEM, the discontinuities are regularized, so to introduce an additional internal length in the description. Moreover, a suitable variational formulation is adopted, based on the concept of the equivalent strain proposed in [5]. A wide range of loading cases and types of reinforcement is considered to prove the generality of our approach. In particular, we show some of the results obtained for the three-dimensional simulation of:

- the pull-out of steel bars embedded in concrete blocks;
- single-lap shear tests where the detachment of FRP plates glued to the concrete blocks occurs;
- three point bending tests on concrete beams externally-reinforced by FRP-plates.

2 BASIC RELATIONSHIPS OF THE REGULARIZED XFEM

The proposed approach has several advantages that make it suitable for modeling mechanical problems such as pull-out and delamination. Firstly, the model is enriched with a regularization length that governs the width of the process zone. This feature avoids the possible dependency on the mesh-size adopted within the zone where strain localization occurs. For instance, this drawback occurs when softening constitutive laws are adopted for the concrete. Secondly, a smooth continuous-discontinuous transition is obtained [6]. Thirdly, the regularized XFEM is based on a damage law that can correctly reproduce both the opening and the shearing modes characterizing the debonding of the FRP layer from the concrete. A thorough numerical investigation on single-lap shear tests has been presented in a recent paper [1].

The basic relationships of the regularized XFEM approach are shown hereinafter. Let the displacement field $\mathbf{u}$ be discontinuous across the failure surface defined according the mechanical problem $\mathcal{S} \in \mathbb{R}^3$ of normal $\mathbf{n}_S$. Within a single element of nodal degrees of freedom $\mathbf{U}^e$ and $\mathbf{A}^e$ interpolated by the usual FE interpolation functions $\mathbf{N}^e$, the regularized XFEM displacement $\mathbf{u}^e$ of element e is [4]

$$\mathbf{u}^e = \mathbf{N}^e\mathbf{U}^e + \mathcal{H}_\rho\mathbf{N}^e\mathbf{A}^e\,, \tag{1}$$

where $\mathcal{H}_\rho$ is a regularized Heaviside function that approximates the Heaviside function for vanishing regularization length ρ. The vector $\mathbf{A}^e$ collects the jump components along x, y and z for the finite element e. $\mathcal{H}_\rho$ is assumed a function of the distance from the level set surface. By compatibility, the strain field is

$$\boldsymbol{\varepsilon}^e = \mathbf{B}^e\mathbf{U} + \mathcal{H}_\rho\mathbf{B}^e\mathbf{A}^e + \|\nabla\mathcal{H}_\rho\|(\mathbf{N}^e\mathbf{A}^e \otimes \mathbf{n}^e)\,, \tag{2}$$

where $\mathbf{B}^e = \nabla\mathbf{N}^e$ is the standard FE compatibility matrix.

FRP and adhesive are modeled as linear elastic materials. At each Gauss point, we introduce the damage variables D and D_c for the concrete and the zone where debonding occurs, respectively, and compute the associated stresses thorough

$$\boldsymbol{\sigma}^e = (1-D)\mathbf{E}\,\mathbf{B}^e\mathbf{U} + \mathcal{H}_\rho\,(1-D)\mathbf{E}\,\mathbf{B}^e\mathbf{A}^e\,, \tag{3a}$$

$$\boldsymbol{\sigma}_c^e = (1-D_c)\mathbf{E}_c\|\nabla\mathcal{H}_\rho\|(\mathbf{N}^e\mathbf{A}^e\otimes\mathbf{n}^e)\,. \tag{3b}$$

In particular, the concrete damage D is governed by an exponential Rankine elasto-damaging

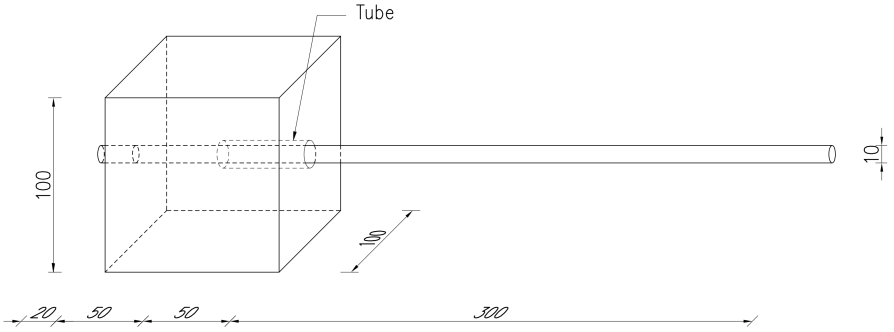

Figure 1: Pull-out: Geometry of the pullout test [7]

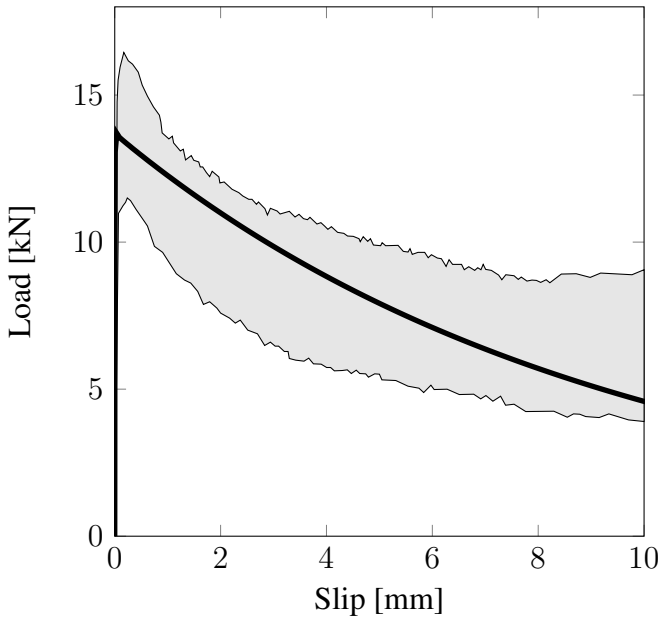

Figure 2: Pull-out: Numerical and experimental load vs slip curves with plain rebars

law until it has reached the critical value D^{cr} [6]. As soon as $D \geq D^{cr}$, the evolution of D is dropped, i.e. the concrete can only elastically unload: a regularization zone replaces the discontinuity. In particular, the damage evolution can be D_c affecting the stress $\boldsymbol{\sigma}_c^e$ is

$$D = \min\{D^{cr}, f(r)\}\,, \quad D_c = \max\{D^{cr}, f(r)\}\,, \quad f(r) = 1 - \frac{r_0}{r_c}\exp\!\big(-2\,H\frac{r_c - r_0}{r_0}\big)\,, \tag{4}$$

where $r_c \geq r_0$, with $r_0 = f_t$ for tensile damage, and $r_0 = f_c$ for compressive damage.

The stiffness matrix associated with the variational formulation is

$$\mathbf{K}^e_{reg} = \begin{bmatrix} \mathbf{B}^{et}\,(1-D)\mathbf{E}\,B_u & \mathbf{B}^{et}\,\mathcal{H}_\rho(1-D)\mathbf{E}\,\mathbf{B}^e \\ \mathbf{B}^{et}\,\mathcal{H}_\rho\mathbf{E}\,\mathbf{B}^e & \mathbf{B}^{et}\,\mathcal{H}^2_\rho(1-D)\mathbf{E}\mathbf{B}^e + \|\nabla\mathcal{H}_\rho\|\bar{\mathbf{N}}^{e\,t}(1-D_c)\mathbf{E}_c\bar{\mathbf{N}}^e \end{bmatrix}. \quad (5)$$

In Eq. (5), the operator $\bar{\mathbf{N}}^e$ is such that $\nabla\mathcal{H}_\rho \otimes \mathbf{N}^e A \approx \|\nabla\mathcal{H}_\rho\|\bar{\mathbf{N}}^e\mathbf{A}_e$, and $\nabla(\mathcal{H}_\rho\mathbf{N}^e) = \mathcal{H}_\rho\,\mathbf{B}^e + \nabla\mathcal{H}_\rho \otimes \mathbf{N}^e$. The adopted variational formulation has been thoroughly described in [5].

3 PULL-OUT

In this section, the regularized XFEM approach is employed to investigate the behavior of the bond between concrete and steel rebars. For a comparison with experimental results, we have considered the experimental campaign of Xiao et al. [7], where several pullout tests with plain and deformed bars were carried out. Fig. 1 shows the pullout test specimens. According to the experimental test, the load was monotonically increased. The applied load versus the slip measured at the free end of the steel rebar have been detected. The numerical and the experimental results are compared in Fig. 2, where the gray zone indicates the experimental results. The agreement between the results is very satisfying.

4 SINGLE-LAP SHEAR TESTS

Two single-lap-shear tests have been simulated, where an axial pulling force is applied to an FRP-plate that is glued to a concrete block restrained by a suitable supporting system. Consistently with the experiments, a layer comprehensive of both a concrete layer attached to the FRP plate is modeled.

For a comparison with the experimental results, the experimental test performed by Chajes et al. [8] and the tests carried out by Carrara et al. [9] have been simulated. It is remarkable that, in the former test, the structural response has been recorded up to the maximum load. On the contrary, in the latter test, the entire load-displacement curves with softening post-peak branches have been detected. The geometry and the material parameters of the experimental tests are specified in Tab. (4). The specimens are displayed in Fig. 3. In the geometry adopted by Chajes et al. [8], the glue layer starts at the front of the specimen, close to the loaded end of the FRP plate. On the contrary, in the specimen of Carrara et al. [9], the FRP plate is bonded at a certain distance from the front of the concrete block to avoid the detachment of a concrete wedge when pulling the FRP sheet. The maximum transferable loads computed are shown for variable bonding length in Fig. 4 for both the specimens. Fig. 5 shows a comparison between

	Chajes et al.[8]			Carrara et al. [9]		
	FRP	glue	concrete	FRP	glue	concrete
E [MPa]	108380	1585	33640	168500	3517.3	28700
ν	0.248	0.315	0.2	0.248	0.315	0.2
f_t[MPa]	–	–	3.21	–	–	2.85
thickness [mm]	1.0	1.0	–	1.3	1.3	–
H [mm]	152.4	152.4	152.4	90	90	90
B [mm]	150	150	150	152.4	152.4	152.4
L [mm]	300	300	300	228.6	228.6	228.6
b [mm]	25.4	25.4	25.4	30	30	30

Table 1: Shear tests: Material and geometry parameters [2]

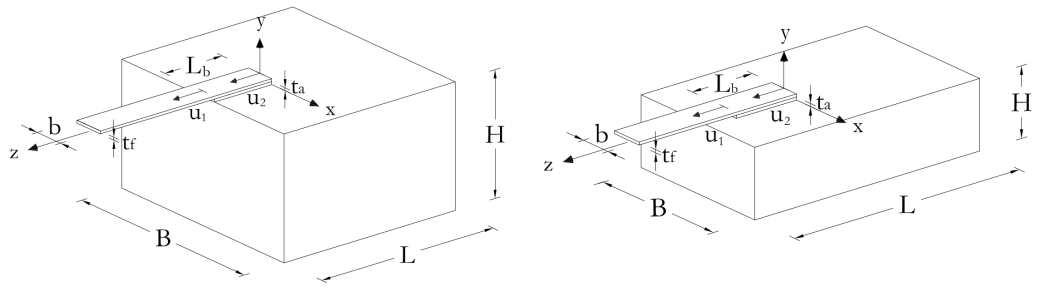

Figure 3: Shear tests: Geometries of the tests of Chajes et al. [8] and Carrara et al. [9]

the numerical displacement contour plot (b) and displacement vectors determined by Czaderski et al. [10] through Image Correlation System (ICS). As evident, the agreement of the computed results with the experimental measured is very satisfying. In particular, this comparison puts into evidence the crucial role played by the bending of the FRP plate during delamination. More results on these single-lap shear tests can be found in our study [1].

5 FLEXURAL STRENGTHENING: THREE-POINT BENDING TEST

In this section, the flexural strengthening carried out by FRP plates bonded to concrete beams has been investigated by means of the regularized XFEM approach. To this purpose, the three-point bending test carried out by Yin et al. [11] was modelled. The geometry of the specimen is reported in Fig. 6. Noteworthy, a steel fiber reinforced concrete was used with short steel-fibers 30 mm long with a diameter of 0.5 mm. An FRP-plate was glued to the bottom of the beam. No steel bars were employed. Concrete with compressive strength $f_{cm} = 26$ MPa, Young's modulus $E_c = 25$ GPa and Poisson ratio $\nu = 0.2$ were employed.

Different volumes of short steel-fibers were mixed with the concrete matrix. In particular, the experimental results obtained using four volume-fractions of short steel-fibers. As known, the mechanical properties of the steel-fiber reinforced concrete change with V_f. Among the available models predicting the improvement of the strength of the concrete with V_f, we adopted the Job et. al. [12] formula

$$f_{spc} = 0.63(f_{cm})^{0.5} + 0.288(f_{cm})^{0.5} R_I + 0.052 R_I \,, \tag{6}$$

where the strength is a function of the fiber reinforced index ($R_I = V_f L_f/\phi_f$), L_f is the length of fiber, and ϕ_f is the diameter of fiber.

In these experiments, the FRP-debonding is due to the concentration of the interfacial shear stress after the occurrence of diffused flexural cracks in the concrete. In Fig. 7, the experimental crack pattern [11] obtained by setting $f_t = 2.89$ MPa, and $H = 0.008$ for $V_f = 0\%$is compared with that obtained with the present regularized XFEM. In particular, the damage variable in the concrete has been plotted, with the red color denoting value of the damage variable close to 1. The evolution of the process of detachment of the FRP plate from the concrete beam is shown in Fig. 8.

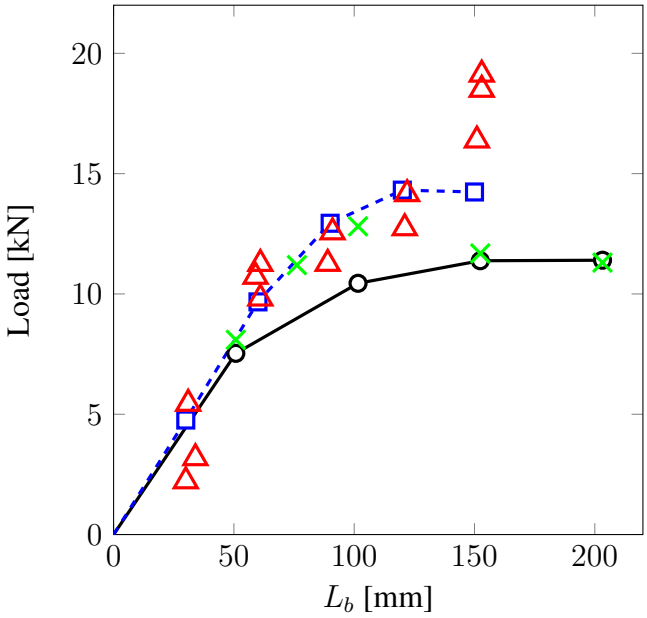

Figure 4: Shear tests: Numerical and experimental maximum lads versus bonding length L_b for the tests of Carrara et al. [9] (numerical data: dashed line and rectangle marker, experimental data: triangle marker) and Chajes et al. [8] (numerical data: continuous line and circle markers [2], experimental data: cross markers).

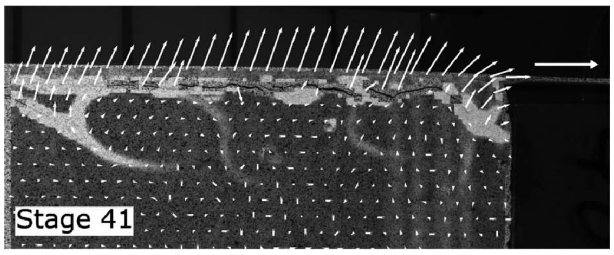

(a)

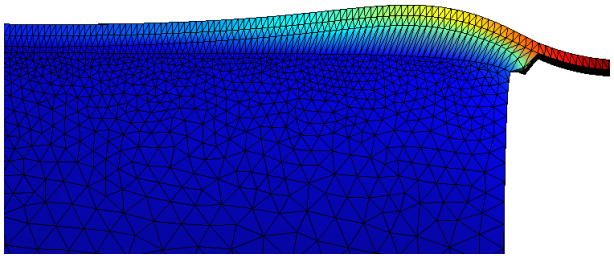

(b)

Figure 5: Shear tests: Qualitative comparison between the numerical displacement contour plot (b) and the displacement vectors (a) determined by Czaderski et al. [10] through a Image Correlation System (ICS).

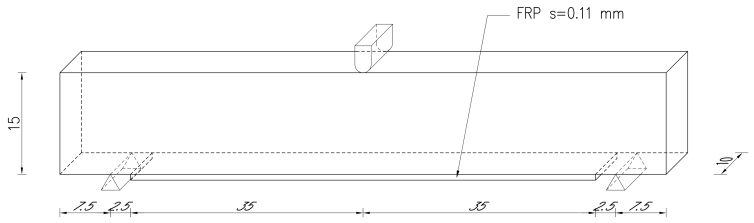

Figure 6: Three point bending test: Geometry of the test carried out by Yin et al.[11]

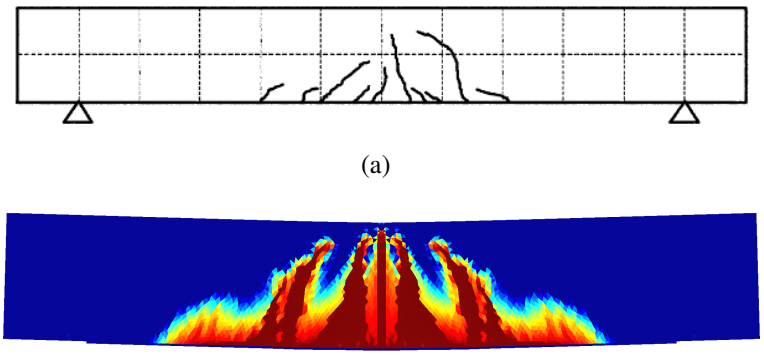

(a)

(b)

Figure 7: Three point bending test: Experimental (a) and numerical (b) crack pattern of the test carried out by Yin et al. [11]

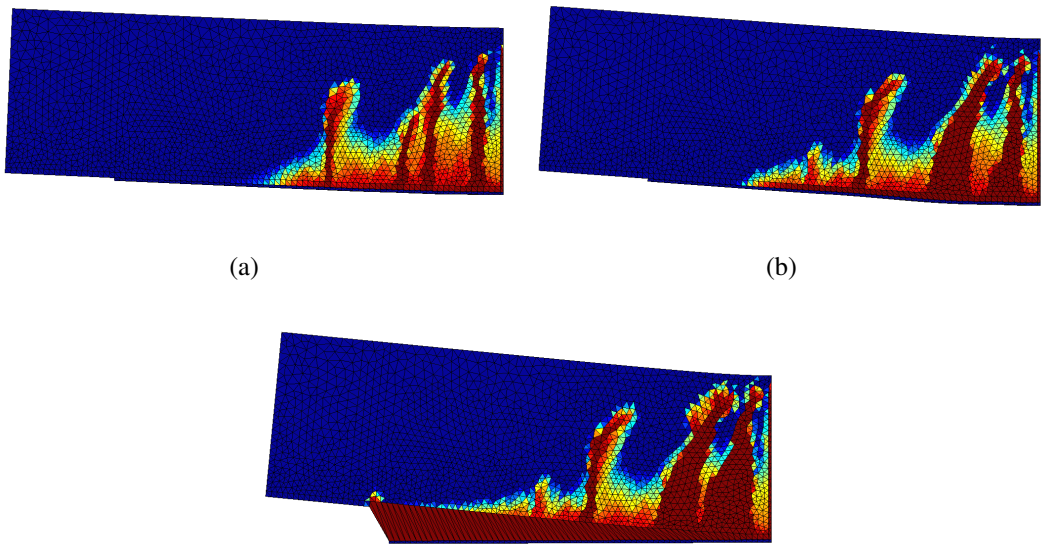

(a) (b)

(c)

Figure 8: Three point bending test: damage evolution up to final delamination

6 CONCLUSIONS

Accounting for both the shearing and the opening of the interface between the reinforcements and the concrete, the regularized three-dimensional XFEM approach has been successfully applied to simulate the debonding of steel rebars and FRP-plates in pull out, shear and bending tests. The proposed approach is able to catch the main features of the structural behavior. The agreement with the reference results is highly satisfying. Hence, the proposed approach can be used together with and in alternative to experimental tests.

REFERENCES

[1] E. Benvenuti, N. Orlando, D. Ferretti, A. Tralli, *A new 3D experimentally consistent XFEM to simulate delamination in FRP-reinforced concrete*, **91**, 346–360, 2016.

[2] E. Benvenuti, O. Vitarelli, A. Tralli, Delamination of FRP-reinforced concrete by means of an extended finite element formulation. *Composites Part B: Engineering*, **43.8**, 3258–3269, 202.

[3] E. Benvenuti, G. Ventura, N. Ponara, A. Tralli, Variationally consistent eXtended FE model for 3D planar and curved imperfect interfaces. *Computer Methods in Applied Mechanics and Engineering*, **267**, 434–457, 2013.

[4] T. Belytschko, R. Gracie, G. Ventura, A review of extended/generalized finite element methods for material modeling, *Modelling and Simulation in Material Science and Engineering*, **17.4**, 043001, 2009.

[5] E. Benvenuti, XFEM with equivalent eigenstrain for matrix–inclusion interfaces. *Computational Mechanics*, **53.5**, 893–908, 2014.

[6] E. Benvenuti, A. Tralli, Simulation of finite-width process zone for concrete-like materials, *Computational Mechanics*, **50**, 479–497, 2012.

[7] J. Xiao, H. Falkne, Bond behaviour between recycled aggregate concrete and steel rebars. *Construction and Building Materials*, **21**, 395–401, 2007.

[8] MJ. Chajes, WW. Finch Jr, TF. Januszka, TA. Thomson Jr, Bond and force transfer of composite material plates bonded to concrete, *ACI Structural Journal*, **93**, 209–217, 1996.

[9] P. Carrara, D. Ferretti, F. Freddi, G. Rosati, Shear tests of carbon fiber plates bonded to concrete with control of snap-back. *Engineering Fracture Mechanics*, **15**, 2663–2678, 2011.

[10] C. Czaderski, K. Soudki, M. Motavalli, Front and Side View Image Correlation Measurements on FRP to Concrete Pull-Off Bond Tests *Journal of Composites for Costruction*, **47**, 1326–1336, 2011.

[11] J. Yin, Z.S. Wu, Structural performances of short steel-fiber reinforced concrete beams with externally bonded {FRP} sheets. *Construction and Building Materials*, **17**, 463–470, 2007.

[12] T. Job, R. Ananth, Mechanical properties of steel fiber-reinforced concrete. *Journal of materials in civil engineering*, **19**, 385–392, 2007.